On Bouncing Oil Drops

A Thesis
Presented to
The Division of Mathematics and Natural Sciences
Reed College

In Partial Fulfillment
of the Requirements for the Degree
Bachelor of Arts

Miguel B. Conner

May 2015

Approved for the Division
(Physics)

Daniel Borrero

Blog

This is the portion of the thesis that I will update regularly with rough notes, lit reviews, results, etc. some of which will be worked in to the real document after some polishing.

0.1 Goals

- 10/14: Define specific problem.
- By Winter Break: Lit Review Complete
- Before Spring Break: Take Data

0.2 To Do

- Figure out citations. 12/23/14
- Take Sample Data Run. Migul 12/2/14
- Learn de Broglie's interpretation of QM. Miguel 11/6/14

0.2.1 Done

- Set up Accelerometer (Finally–ugh). Miguel 2/20/15
- Get New Silicone Oil. Miguel 1/10/15
- Send copy of Lit Rev to Daniel to proofread. 12/23/14
- Find walking regime. Miguel 11/20/14
- Order Accelerometer. Miguel 11/6/14
- Learn Basics of Bohmian Mechanics. Miguel 10/28/14
- Make tray. Miguel 10/20/14
- Sort out camera situation. Miguel 10/20/14

- Obtain flashdrives. Miguel 9/30/14
- Learn how to use the new LaTeX and Github setup. Miguel 9/30/14

0.3 Literature Review

(Important: Particle-wave association on a fluid interface (Protiere 2006)).

In 2005, Yves Couder showed that bouncing oil drops on vertically vibrating fluid bath exhibited properties analogous to the paradoxical properties seen only at the quantum scale (CITE: Dynamical phenomena: Walking and orbiting droplets?). Couder, John Bush, and others have shown that this system can reproduce double-slit single-particle interference, orbiting, tunneling, quantized orbits, spin, and more. The trajectory of the droplet can be modeled mathematically, and the dynamics of the walker have similarities to de Broglie's theory of quantum mechanics (CITE: Bush 2015).

The literature review will begin with a description of Faraday waves and the basic dynamics of a bouncing droplet and a walking droplet. Then we will describe in detail a few of the important quantum-like properites of this system.

0.3.1 Faraday Waves

?

0.3.2 Bouncing Droplets

Though it had been around for at least a century, the phenomena of droplets bouncing on a vibrating fluid bath was first explained by Jearl Walker in 1978 CITE: WALKER. The first experiments looked at water droplets (bouncing on a vibrating water bath) that persisted for several seconds. Adding detergent to the water and modifying the frequency of vibration increased droplet's lifetime to minutes. Conversely any particulate impurities descrease the droplet's lifetime. Walker concluded that the droplets failed to coalesce because a layer of air trapped between the droplet and the bath would keep the two separate.[1] In other words, the droplet bounces on a cushion of air.

0.3.3 Walking Droplets

It was Couder who then showed that an oil droplet could live for much longer. Long lifetimes meant that the focus could shift from how the doplet bounced (short time scale) to its interactions with other droplets and its motion (longer time scale).

Every time the droplet impacts the bath, it creates a radial traveling wave. If the bouncing droplet impacts the wavefield in such a way that it recives a lateral force from the slope of the wave, then it will be pushed to the side slightly. The next time

[1] Reedie ??? wrote his thesis titled: "???" on this very topic!

the droplet makes contanct with the bath, it will again make contact with a slope, and be pushed to the side. This propels the bouncing droplet, causing it to "walk" across the surface of the bath. These "walkers" turned out to have particularly interesting behaviours. Indeed, in 2006 Yves Couder and Emmanuel Fort showed that these droplets mimicked the behavior of electrons in the hallmark experiment of quantum weirdness: the double slit experiment. This was the first time that microscopic scale behavior had ever been seen at a macroscopic level, and it sparked interest in the experiment.

0.3.4 Macroscopic Quantum Scale Behaviors

Basic Parameters

Consider a fluid of density ρ, viscosity ν, and surface tension σ, in a bath of depth H driven vertically at an amplitude A_0 at frequency $f = \omega/2\pi$. By defining $\gamma = A_0\omega^2$, the effective gravity in the frame of reference of the bath is $g + \gamma \sin(\omega t)$.

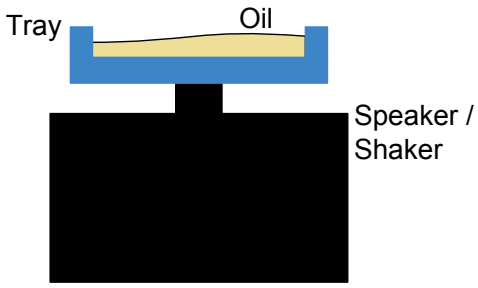

Figure 1: The experimental setup. The tray vibrates with an amplitude A_0.

The oil droplet of diameter D bounces in the regime $\gamma < \gamma_F$, where γ_F is the Faraday threshold (at this point, Fraday waves appear). The important experimental limits are outlined in Table 1.

Table 1: Approximate Limits for Bouncing Drop Behavior

Parameter	Lower Limit	Upper Limit
Viscocity ν (cSt)	10	100
Bath Depth H (mm)	4	10
Frequency f (Hz)	20	150
Amplitude A_0 (mm)	0.1	1
Drop Diameter D (mm)	0.6	1.0

For certain parameters, the bouncing drop will behave differently. The vibration number describes "the relative magnitude of the forcing frequency and the drop's

natural oscillation frequency," and is given by:

$$V_i = \frac{\omega}{2}\sqrt{\frac{\rho D^3}{2\sigma}} \tag{1}$$

The natural frequency of the droplet occurs around $V_i = 0.65$, where the droplet can exhibit both walking and bouncing behaviors. Setting up a plot with V_i on the y axis and (dimensionless) γ/g on the x axis can help in showing the behavior of the droplet, shown in Fig. 2.

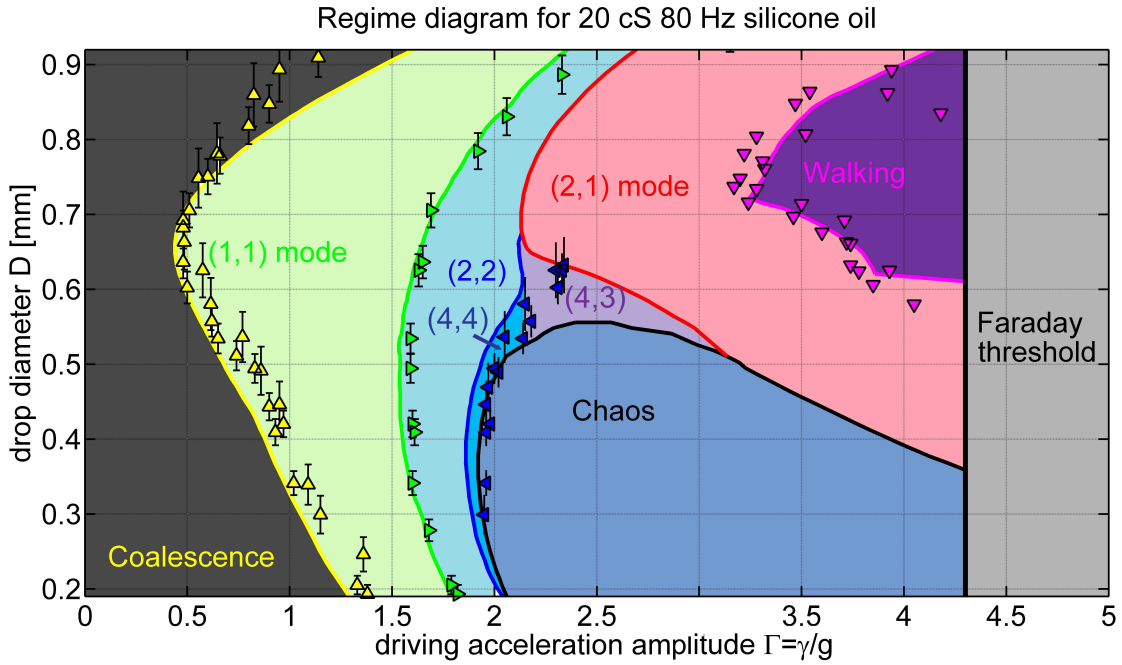

Figure 2: The different bouncing regimes for the oil drops of 20 cS silicon oil and at $f = \omega/2\pi = 80$ Hz. The parameters (m,n) describe the droplet that bounces n times in m forcing periods.

The various modes seen in Fig. 2 can be described by (m,n), where n is the number to times the droplet contacts the surface over period m/f. For example, in the (1,1) mode, the droplet hits the oil bath once per driving period. In the (2,2) mode, the drop makes two bounces of differing heights.

0.3.5 Path Memory

Path memory is a parameter that can be varied in this setup; it is essentially the damping of the system. Every time the droplet impacts the bath, it creates a radial traveling wave. Over the course of many bounces, a wavefield composed of a superposition of the many waves arises. In this way the wavefield "remembers" previous interactions. Because droplet motion is influenced by the wavefield, controlling the damping of the wavefield will influence the path of the walker. The heavily damped system has a low memory, while undamped system corresponds to higher memory.

As one gets closer to the Faraday threshold, one achieves higher and higher memory because waves last for longer. The quantum like features of this experiment arise in the high-memory limit. (For more, Eddi et. al, 2011b: Information stored in Faraday waves.)

0.3.6 Bound States

A bouncing droplet creates a damped wave that depends on the driving acceleration (γ_m/g) CITE: Protiere 2005. A periodic damped wave allows for two bouncers to form a "bound state". Starting far away from one another, the two droplets drift towards one another until a fixed distance d_0^{bd}. Increasing driving acceleration will decrease the value of d_0^{bd}. These bound bouncers form triangular lattices, and their periodicity is highly sensitive to the mass of the droplet. (LOOK AT EDDI ET ALL 2008).

Walkers can also form bound states. Two walkers of the same size that are approaching one another can form an orbit around their center of mass. Between the two droplets is the fixed distance d_n^{orb} given by

$$d_n^{orb} = (n - \epsilon_0)\lambda_F \tag{2}$$

where ϵ_0 is a fixed distance which is the same for all orbitals of these walkers (usually in the range $0.15 < \epsilon_0 < 0.25$ depending on droplet diameter), and $n = 1, 2, 3...$ for drops that are in phase or $n = 1/2, 3/2, 5/2...$ for drops out of phase. Orbiting periods are approximately porpotional to d_n^{orb}, which ends up meaning that the velocity of the orbiting walkers is a little less than the velocity of a free walker CITE: Protiere 2006. Orbiting of different sized droplets can also arise.

0.3.7 Scattering States

Two identical walkers headed towards each other can form fixed orbits, or they can scatter. The droplets are deflected through their wavefields (they never actually make contact with one another)

0.3.8 Single-Particle Diffraction

In 2006 Couder and Fort showed that the system had properties that were strikinly similar to two famous and controversial quantum experiments (Couder and Fort, 2006). They were able to demonstrate that a single walker travelling through one slit seemed to have its direction altered seemingly randomly, before continuing forward on its new path. By statistically analyzing many trials, Couder and Fort showed that the histogram of the "diffraction" actually resulted in a diffraction pattern strikingly similar to the single photon diffraction experiment performed by Taylor in 1909.

Next, Couder and Fort added a second slit next to the first one. Now a single walker could pass through one of two slits, and it was discovered that a histomgram of this data returned another diffraction pattern. This result is of course reminiscent

of one of the most famous experiments in physics: Young's double slit diffraction with photons and electrons.

Using a numerical simulation, Couder and Fort were able to reproduce similar results.

As Couder and Fort mention in their paper: "A discussion of the relation between these single-particle experiments and those concerning elementary particles is unavoidable." Important differences and similarities are then described between the quantum system and the quantum-like system. For the differences: we have a dissapative system, where energy is continually put in through the vibration of the tray; the particle can be followed;[2] it's really effectively moving in two dimensions; the velocity is measurable; and the probability distributuion is linked with the wave amplitude (rather than it's intensity). And then of course, the similarities: an uncertainty priciple arises from the statistical data (and without knowledge of the actual paths followed by the walkers); and some others that were unclear...

Recently, Harris attempted to reproduce single slit interference. With better technology, new results were found. Using a looping guiding batt, trajectories were found to follow the same loop without deviating. Only at a very high memory were there chaotic paths.

0.3.9 Tunneling

The guiding wave field can be partially reflected off of an edge or even a change in depth of the oil bath. This effect can be seen when a walker is pushed back from a under-the-surface step, seemingly without any contact. In rare cases, the walker will actually tunnel across the step; that is, it will continue to walk along the surface of the oil bath and pass over the step without reflection. In the first experiment done by Eddi et al., they demonstrated tunneling by by building square "corrals" of varying thicknesses. In the second experiment, they built a rhombus shape which forced the walker across the center of a rhombus. The barrier was placed perpendicular to the direction of travel of the walker, so that it would hit the wall directly rather than at an angle (as in the square corral). "The tunneling probability decreases exponentially with the barrier width and increases as the Faraday threshold is approached." Eddi et. al also found that the probability of tunneling increased with the velocity of the walker. (For more, Eddi et. al 2009b: Unpredictable Tunneling of a classical wave-particle association.)

The unpredictability of the tunneling comes from the complex interatction between the drop and its guiding wave.

0.3.10 Motion in a Confined Geormetry

By tracking the droplet as it bounces around the tray over a period of time, one can look at the overall statistical behavior of the droplet. Two experiments tracked

[2] C and F note that it'd be impossible to dectect the particle without disturbing it "by any means at its scale," like a bouy, for example. As the bouy floated it would interfere with the system by altering the wave pattern on the surface.

walkers in an experimental coral (Harris and Bush, 2013, Harris et al. 2013) in the high-memory, chaotic motion regime. A histogram of the statistical data shows that the "probability of finding a walker at a given point in the corral is roughly prescribed by the amplitude of the Faraday wave mode of the cavity at the prescribed forcing frequency."

Quantum corral experiments performed by Crommie et al. (Crommie et al. 1993 a b) present similar findings. In the experiment, electrons were confined in a Cu(III) substrate using barriers of iron adatoms. Using tunneling spectroscopy, the electrons were found to have a specific resonances depending on the corral shape. As in the case of Harris' circular corral experiment where the corral and the Faraday wavelength, λ_F, dictate the wavelike statistical patter, in the quantum experiment the corral and the *de Broglie* wavelength, λ_{dB}, dictate the form of the wavelike statistical pattern.

0.3.11 Walker Trajectories

In the regime of walkers we have $R_e \sim 20$, $B_0 \sim 0.1$, and $W_e \sim 0.1$. For the millimeric walkers, the dominant force comes from impact of the curvature of the surface. Gilet and Bush (2009: Chaotic bouncing of a drop on a soap film, and the fluid trampline: droplets bouncing on a soap film) show that the surface of the vibrating oil can be modeled with a soap film, where the soap film acts like a linear spring.

As the oil bath is forced up and down, a tiny droplet of oil will "walk" across the surface. Moláček and Bush have developed an equation of a droplet that describes the trajectory of the walking droplet, ignoring the verical dynamics by time averaging them out (cite: J. Moláček and J. W. M. Bush, "Drops walking on a vibrating bath: towards a hydrodynamic pilot-wave theory" J. FluidMech. 727, 612-647 (2013).). The trajectory of the walking droplet of mass m at position $\mathbf{x}(t) = (x(t), y(t))$ is given by

$$m\ddot{\mathbf{x}} + D\dot{\mathbf{x}} = -mg\nabla h(\mathbf{x}, t) \tag{3}$$

where D describes the drag coefficient and $h(\mathbf{x}, t)$ describes the shape of the wavefield. Thus the second term describes the time averaged drag from both the flight and the impact of the droplet (as usual, depends on the velocity), and the third term describes the propulsive wave force resulting from drops landing on the inclined wave surface.

The wavefield is quite complicated because it depends on the memory. For a single impact of a droplet, Oza et al. argue the surface wave can be approximated with an integral of a monochromatic radial Bessel function of the first kind

$$h(\mathbf{x}, t) = \frac{F}{T_F}\int_{-\infty}^{t} J_0 \frac{(k_F|\mathbf{x}(t) - \mathbf{x}(s)|)}{|\mathbf{x}(t) - \mathbf{x}(s)|}(\mathbf{x}(t) - \mathbf{x}(s))e^{-(t-s)/(T_F M_e)}ds \tag{4}$$

with F giving the wave force coefficient (estimated in the above source), T_F describing the Faraday period, and k_F describing the Faraday wave number determined by the Faraday wavelength $\lambda_F = 2/k_F$ (integral from A. U. Oza, D. M. Harris, R. R. Rosales, and J. W. M. Bush, "Pilot-wave dynamics in a rotating frame: on the emergence of orbital quantization" J. Fluid Mech. 744, 404-429 (2014).). (Faraday was a popular

guy.) Finally, that last term M_e is the nondimensional memory parameter $M_e = T_d/[T_F(1-\gamma/\gamma_F)]$ (with T_d being the unforced decay time).

0.4 Experimental Setup

0.5 Bohmian Mechanics

0.5.1 Formalism

The Schroedinger Equation and ψ

We begin with the Schoedinger equation

$$i\hbar\frac{\partial}{\partial t}\psi = \hat{H}\psi \tag{5}$$

where $\hat{H}$ is the Hamiltonian and ψ is the wavefunction. The Hamiltonian can be expanded (assuming there is no electric field) to give

$$i\hbar\frac{\partial}{\partial t}\psi(\mathbf{x},t) = \left[\frac{-\hbar^2}{2m}\nabla^2 + V(\mathbf{x},t)\right]\psi(\mathbf{x},t) \tag{6}$$

where $V(\mathbf{x},t)$ is the potential energy of the system. The solution ψ is of the form:

$$\psi(\mathbf{x},t) = R(\mathbf{x},t)e^{iS(\mathbf{x},t)/\hbar} \tag{7}$$

where S and R are real. Plugging in our equation for ψ into the Schoedinger equation (Eq. (6)) will produce two separate equations: one giving the time derivative of R and the second giving the time derivative of S. From these equations, a Hamilton-Jacobi equation can be written for a quantum system. Let's begin by computing the left hand side of Eq. (6) in terms of R and S.

$$\begin{aligned} i\hbar\frac{\partial}{\partial t}\psi(\mathbf{x},t) &= i\hbar\left(\frac{\partial R}{\partial t}e^{iS/\hbar} + R\frac{i}{\hbar}\frac{\partial S}{\partial t}e^{iS/\hbar}\right) \\ &= i\hbar\left(\frac{1}{R}\frac{\partial R}{\partial t} + \frac{i}{\hbar}\frac{\partial S}{\partial t}\right)\psi(\mathbf{x},t) \\ &= \left(i\hbar\frac{1}{R}\frac{\partial R}{\partial t} - \frac{\partial S}{\partial t}\right)\psi(\mathbf{x},t) \end{aligned}$$

Let's leave that alone for a little bit, while we focus on the right hand side of Eq. (6). Since it's a little more complicated, we will start with one term of the right hand side:

$$\begin{aligned} \nabla^2\psi(\mathbf{x},t) &= e^{iS/\hbar}\nabla^2 R + \left(\frac{i}{\hbar}\right)^2(\nabla S)^2 R e^{iS/\hbar} + \left(\frac{i}{\hbar}\right)Re^{iS/\hbar}(\nabla^2 S) + \left(\frac{2i}{\hbar}\right)(\nabla R\cdot\nabla S)Re^{iS/\hbar} \\ &= \left(\frac{\nabla^2 R}{R} - \left(\frac{\nabla S}{\hbar}\right)^2 + \left(\frac{i\nabla^2 S}{\hbar}\right) + 2i\left(\frac{\nabla R\cdot\nabla S}{\hbar}\right)\right)\psi(\mathbf{x},t) \end{aligned}$$

Now the hard part is done, and we can say that the right hand side of Eq. (6) is given by

$$\left[\frac{-\hbar^2}{2m}\nabla^2 + V(\mathbf{x},t)\right]\psi(\mathbf{x},t) = \left[-\frac{\hbar^2\nabla^2 R}{2mR} + \left(\frac{(\nabla S)^2}{2m}\right) - i\hbar\left(\frac{\nabla^2 S}{2m}\right) - i\hbar\left(\frac{\nabla R\cdot\nabla S}{m}\right) + V(\mathbf{x},t)\right]\psi($$

Ok, now that we've got that done, the next part will be super easy. Starting with Schrodinger's equation and plugging in left and right hand sides we calulated seperately.

$$i\hbar\frac{\partial}{\partial t}\psi(\mathbf{x},t) = \left[\frac{-\hbar^2}{2m}\nabla^2 + V(\mathbf{x},t)\right]\psi(\mathbf{x},t)$$

$$\left(i\hbar\frac{1}{R}\frac{\partial R}{\partial t} - \frac{\partial S}{\partial t}\right)\psi(\mathbf{x},t) = \left[-\frac{\hbar^2\nabla^2 R}{2mR} + \left(\frac{(\nabla S)^2}{2m}\right) - i\hbar\left(\frac{\nabla^2 S}{2m}\right) - i\hbar\left(\frac{\nabla R\cdot\nabla S}{m}\right) + V(\mathbf{x},t)\right]\psi(\mathbf{x},$$

Now we can divide out ψ from both sides

$$i\hbar\frac{1}{R}\frac{\partial R}{\partial t} - \frac{\partial S}{\partial t} = -\frac{\hbar^2\nabla^2 R}{2mR} + \left(\frac{(\nabla S)^2}{2m}\right) - i\hbar\left(\frac{\nabla^2 S}{2m}\right) - i\hbar\left(\frac{\nabla R\cdot\nabla S}{m}\right) + V(\mathbf{x},t)$$

and group the imaginary numbers on the left side and the real numbers on the right side

$$i\hbar\frac{1}{R}\frac{\partial R}{\partial t} + i\hbar\left(\frac{\nabla^2 S}{2m}\right) + i\hbar\left(\frac{\nabla R\cdot\nabla S}{m}\right) = \frac{\partial S}{\partial t} - \frac{\hbar^2\nabla^2 R}{2mR} + \left(\frac{(\nabla S)^2}{2m}\right) + V(\mathbf{x},t)$$

Recall that both S and R are real. Note that the only way for all of the imaginary terms to equal all of the real terms is if they both equaled zero.

$$i\hbar\left(\frac{1}{R}\frac{\partial R}{\partial t} + \frac{\nabla^2 S}{2m} + \frac{\nabla R\cdot\nabla S}{m}\right) = \left(\frac{\partial S}{\partial t} - \frac{\hbar^2}{2m}\frac{\nabla^2 R}{R} + \frac{(\nabla S)^2}{2m} + V(\mathbf{x},t)\right) = 0$$

This then gives us two sepeate equations, one for the time derivative of R and another for the time derivative of S.

$$\frac{\partial R}{\partial t} = -\frac{R}{2m}\left(\frac{\nabla^2 S}{m} - 2\nabla R\cdot\nabla S\right) \tag{8}$$

$$\frac{\partial S}{\partial t} = \frac{\hbar^2}{2m}\frac{\nabla^2 R}{R} - \frac{(\nabla S)^2}{2m} - V(\mathbf{x},t) \tag{9}$$

What does this do for us? Both equations will provide helpful descriptions of our system.

The Quantum Potential

We can rewrite Eq. (9) in a provokative way

$$-\frac{\partial S}{\partial t} = \frac{(\nabla S)^2}{2m} + V(\mathbf{x}, t) + \frac{\hbar^2}{2m}\frac{\nabla^2 R}{R} \tag{10}$$

which should look suspiciously familiar. If I were to tell you that ∇S had units of momentum and $\partial S/\partial t$ units of energy, then this equation would look a lot like a Hamiltonian! The first term takes care of the kinetic energy, the second is the potential energy term, but we have this mysterious third term which we haven't ever encountered in classical mechanics. If we define this term as our "quantum potential"

$$U(\mathbf{x}) = \frac{\hbar^2}{2m}\frac{\nabla^2 R}{R} = \frac{\hbar^2}{4m}\left[\frac{1}{2}\frac{\nabla^2 P}{P} - \frac{(\nabla P)^2}{P^2}\right] \tag{11}$$

then we really *can* think of Eq. (10) as a Hamiltonian with an extra potential term thrown in to make it "quantum." Note that in cases where $\hbar$ is much smaller than the rest of the terms (i.e. not the quantum realm), then this quantum potential term goes away, and we are left with the regular Hamilton equation from classical mechanics.

Recall that when writing a Hamiltonian, the potential terms govern the forces on the particle. For a conservative system, the force is given by F(x) = -$\partial U/\partial x$. If we include a quantum mechanical potential in our Hamiltonian, then this potential must cause a force on the paticle in addition to the one supplied by the $V(x)$ term.

Continuity Equation

Plugging in the probability density $P(\mathbf{x}, t) = R^2(\mathbf{x}, t)$ into Eq. (8) also gives us something quite interesting.

MATH?

which we can finally express as

$$\frac{\partial P}{\partial t} + \nabla \cdot \left(P\frac{\nabla S}{m}\right) \tag{12}$$

In describing the quantum potential term it was mentioned that ∇S can be thought of as momentum, so then from our classical relationship between momentum and velocity $\mathbf{v}(\mathbf{x}, t) = \nabla S/m$ can be thought of as velocity. Then by defining the probability current as $j(\mathbf{x}, t) = P\nabla S/m$ then we recover

$$\frac{\partial P}{\partial t} + \nabla \cdot j(\mathbf{x}, t) \tag{13}$$

known as the continuity equation! This tells us that P is conserved over time.

Finding R and S

Chapter 1

Introduction to Tunneling in QM

1.1 Wavefunction

In classical mechanics, one can describe a particle with six variables: three position indicators (x, y, z), and three momentum indicators (p_x, p_y, p_z). One can find a function to represent variable by making multiple measurements across time, and discover an expression $x(t)$ that describes the particles location in space along the x dimension at time t. When all six variables can be described by a function, one can describe the position of the particle at any time.

In quantum mechanics however, Heisenberg's uncertainty priciple limits the knowledge of position and momentum:

$$\sigma_x \sigma_p \geq \hbar/2.$$

This equation states that as one knows more about the position of the system, then one loses knowledge about the momentum of the system, and vis versa. It's a tradeoff inherent to the nature of the system, not due to experimental deficiences. And it means that the strategy of finding equations for position and momentum of a system are no longer possible. If a particle has no exact position, can one represent where it might be? One can use a wave describing the probability of finding the particle at that position. The square root of this wave is called the wavefunction, and is represented by $\Psi(x,t)$.

1.2 Schroedinger's Equation

The wavefunction $\Psi(x,t)$ is goverened by the Schroedinger equation:

$$i\hbar\frac{\partial}{\partial t}\Psi(x,t) = \left[\frac{-\hbar^2}{2m}\frac{\partial^2}{\partial x^2} + V(x,t)\right]\Psi(x,t)$$

where $V(x,t)$ is the given potential, m is the mass of the particle, and $\hbar$ is the reduced Planck's constant. For potentials that do not change in time, one can use separation

of variables to arrive at the time-independant Schroedinger equation

$$E\Psi(x,t) = \left[\frac{-\hbar^2}{2m}\frac{\partial^2}{\partial x^2} + V(x)\right]\Psi(x,t)$$

where E is the total energy. The goal is to find $\Psi(x,t)$ knowing the potential $V(x)$.

1.3 Barrier Potential

1.4 Energies

1.4.1 $E = V_0$

1.4.2 $E > V_0$

1.4.3 $E < V_0$

1.5 Physics

Many of the symbols you will need can be found on the math page (`http://web.reed.edu/cis/help/latex/math.html`) and the Comprehensive LaTeX Symbol Guide (enclosed in this template download). You may wish to create custom commands for commonly used symbols, phrases or equations, as described in Chapter **??**.

Chapter 2

Experimental Design

To test the effect of a barrier's height on the probability of tunneling, I used a combination of procedures and conventions from the experiments of John Bush, Yves Couder, and specifically, Eddi 2009 (CITE!). These elements were then slightly modified to fit some of the unique features of my experiment. In particular, I aim to give some of the reasoning behind the tray design and data collection techniques, both of which are not well described in the literature.

2.1 Setup

The combined setup is shown in Fig. 2.1.

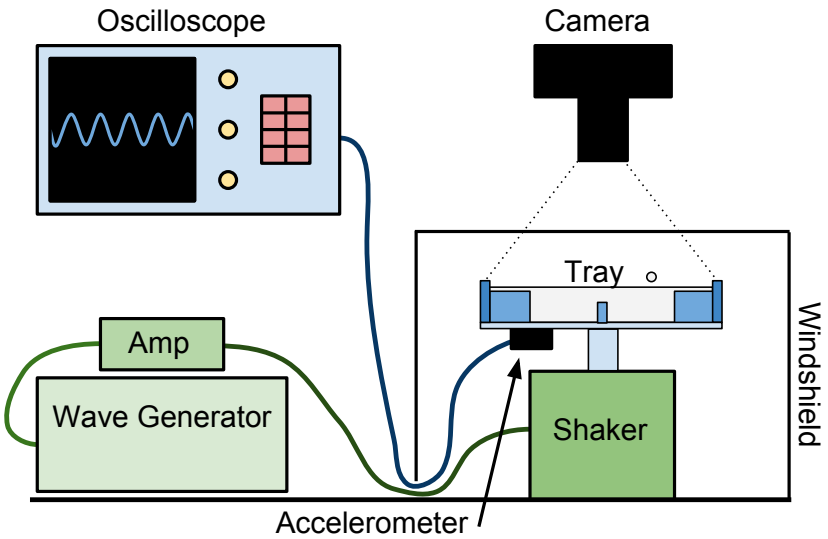

Figure 2.1: The experimental setup. The amplified signal from the wave generator drives the shaker. The accelerometer generates a signal which is read by the oscilloscope. The windshield blocks disturbances to the experiment, while allowing the camera to document the trials.

2.2 Materials

The key components of this experiment are the shaker, the oil, and the tray. In this section I'll describe the specifics of the big three, as well as some of the additional components used in data collection.

2.2.1 Tray

The tray was made of plastic parts machined by the (MODEL NUMBER?) laser cutter. They were then glued together with GLUE?. The tray's design guides the droplet and creates smooth droplet trajectories. The tray schematic is shown in Fig. 2.2.

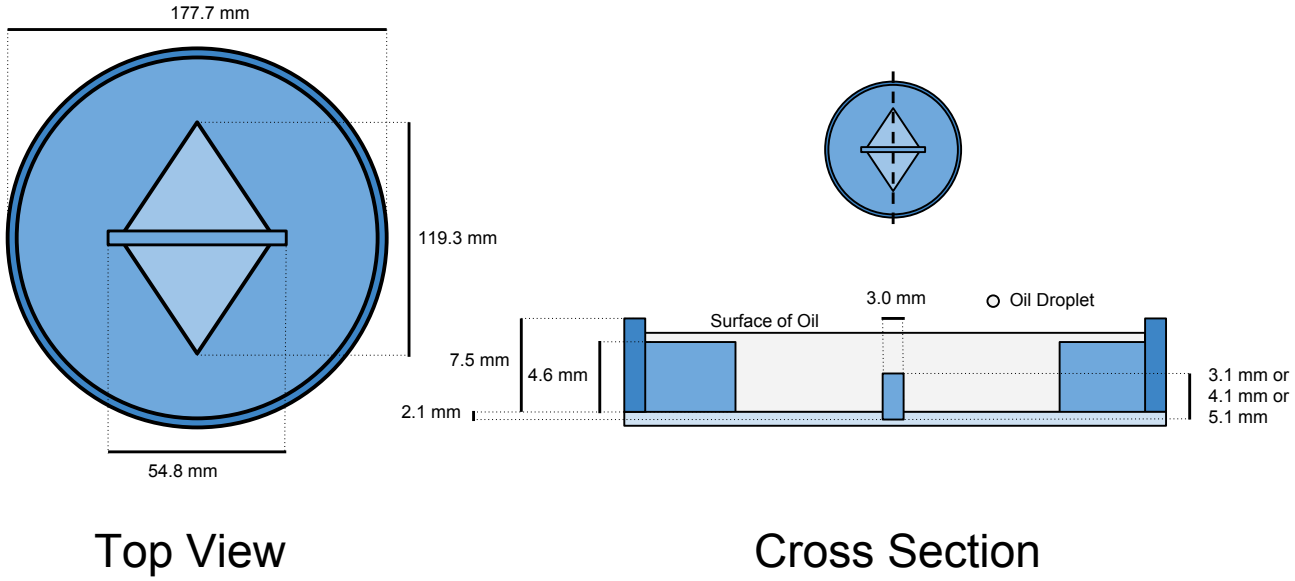

Figure 2.2: The specifications of the tray design. The top view (left) highlights the main elements in the tray, while the cross section (right) illustrates the topography of the tray.

A thin layer of oil spills over the constraining rhombus shape. As long as the layer is thin enough, the droplet will remain in the rhombus container, but the waves will continue to propagate unimpeded. This gives the waves time to decay, and means that the droplets motion isn't chaotically affected by reflections of previous waves and is instead guided by the unreflected waves.

The rhombus shape serves to steer the droplet into a perpendicular collision with the barrier. This works because the droplet will pin-ball its way into the acute corner of the rhombus, and will shoot out in a straight line, directly towards the barrier. (FIGURE of pinballing droplet?)

I designed my experiment to test barriers of three different heights: 2.75 mm, 3.0 mm, and 3.25 mm, measured from the bottom of the rhombus. A thin barrier of plastic made by the laser cutter has the tendancy to bend and warp over time.

The solution to this problem was to make these barriers taller than the specified heights, and create an cut-out in the rhombus so they could be inserted. The barrier cut-outs were deep enough to exactly counter the added height of the barrier, so the barriers still had (when measured from the surface of the rhombus) heights of 2.75 mm, 3.0 mm, and 3.25 mm. This also solved the problem of fixing the barriers in place, but still making them easily removable. These heights were chosen because they allowed for both passage over and blockage by the barriers. At the lowest heights, most droplets will cross over, where as taller barriers will block most droplets.

The bottom of the tray was painted black in order to provide contrast, which allows the droplet to be more easily tracked by eye and by camera.

2.2.2 Silicon Oil

The silicone oil used in this experiment had a viscosity of 20 cSt (the thickness is a little closer to water than olive oil) obtained from Clearco Products Co., Inc. (CAS No: 63148-62-9). The 20 cSt viscosity of Bush's group was used (over the 50 cSt viscosity of Couder's) because it has a larger walking regime than at other viscosities. The tray requires about x amount of fluid.

It is of vital importance to keep the oil as clean as possible because it keeps the droplet bouncing for longer. This means protecting both from particulate matter that is already in the tray and from the particulate matter that might float on to the surface of the oil. Contamination can be minimized by cleaning the tray before pouring the oil in.

2.2.3 Shaker

To shake the tray, we used a mechanical wave driver made by Pasco Scientific, model SF-9324. This shaker was designed to drive a string or an elastic cord, not a 200 gram tray with oil inside, which was probably at the limit of what the shaker can handle.

2.2.4 Accelerometer

Knowing the tray's acceleration allows us to characterize the behavior of our system using Fig. 2. To measure acceleration, we attached an ADLX 326 triple axis accelerometer to the bottom of the tray. The method of attachment was screws, since it provided a much firmer yet more removable hold than tape or glue. The accelerometer has a range of $\pm 16g$, perfect for measuring the accelerations in our setup, which average about $5g$'s.

The signal from the z-axis of the accelerometer was output directly into the oscilloscope. For the vibrating tray, the output was approximately sinusoidal (as expected). The spec sheet for the accelerometer indicates that the sensitivity can be translated to 57 ± 6 mV/g.

2.2.5 Waveform Generator and Amplifier

The shaker was driven with the Agilent Arbitrary Waveform Generator model 33210, which was controlled digitally and thus created consistent waves.

Adding a Lepai LP2020A+ digital amplifier to the wavefunction generator meant the amplitude of the tray could be precisely controlled.

2.2.6 Windshield

A large, see-through cylinder (covered at one end) was manufactured by the laser cutter. When placed over the tray, it served the purpose of keeping the oil clean from particulate matter and preventing wind currents from influencing the motion of the walker.

2.2.7 Leveling Platform

A leveling platform was made out of wood, with three adjustments to adjust the tilt. This ensured that the tray was always flat. A level placed inside the tray (before the oil was added), ensured the

2.2.8 Camera

2.3 Procedure

2.3.1 Finding the Walking Regime

Before investigating the rate of tunneling using different barriers, a rough estimate of the walking regime at a frequency of 80 Hz must be made to ensure correct behavior. A "map" similar to the one in Fig. 2 will be made, but rather than looking at all of the different kinds of bouncing we will limit ourselves to only the walking regime. Reproducing this figure allows us to find the parameters that are specific to our unique system, which could have slightly different height, tray, oil, and shaker configurations than those used in the literature.

Droplet size is measured using a recorded video of the walking droplet in motion. By comparing the number of pixels making up the diameter of the droplet (unknown measurement) to the number of pixels making up the diameter of the tray (known measurement), we can estimate the "length" of each pixel, and thus find the diameter of the droplet in centimeters.

Driving acceleration values are measured by the accelerometer and displayed by the oscilloscope.

To ensure that every trial has the same oil depth, we must measure the volume of the oil before filling the tray. Knowing the volume of the tray and of each barrier, we can get a value for the oil depth without interfering with the system.

2.3.2 The Experiment

Tunneling was examined for three different barrier heights. At each height (and at a constant frequency of 80 Hz and constant driving acceleration), a string of continuous collisions were filmed with the camera. From this data, a fixed base tunneling "probability" was calculated, which provides the most simplistic analysis of this system.

The tray is designed such that most of the droplet's collisions with the barrier occur "head on" (i.e. perpendicular to the length of the barrier), but not all collisions unfold ideally. A more involved analysis in *Tracker* requires looking at the component of velocity of the droplet perpendicular to the length of the barrier, and determining the probability of tunneling given this value. Since not all collisions in the simplistic analysis occur at the same velocity, this method allows for a more methodical analysis of the phenomena.

Conclusion

Here's a conclusion, demonstrating the use of all that manual incrementing and table of contents adding that has to happen if you use the starred form of the chapter command. The deal is, the chapter command in LaTeX does a lot of things: it increments the chapter counter, it resets the section counter to zero, it puts the name of the chapter into the table of contents and the running headers, and probably some other stuff.

So, if you remove all that stuff because you don't like it to say "Chapter 4: Conclusion", then you have to manually add all the things LaTeX would normally do for you. Maybe someday we'll write a new chapter macro that doesn't add "Chapter X" to the beginning of every chapter title.

4.1 More info

And here's some other random info: the first paragraph after a chapter title or section head *shouldn't be* indented, because indents are to tell the reader that you're starting a new paragraph. Since that's obvious after a chapter or section title, proper typesetting doesn't add an indent there.

Appendix A

The First Appendix

An appendix full of awesome

Appendix B

The Second Appendix, for Fun

An appendix full of win

References

Angel, E. (2000). *Interactive Computer Graphics : A Top-Down Approach with OpenGL*. Boston, MA: Addison Wesley Longman.

Angel, E. (2001a). *Batch-file Computer Graphics : A Bottom-Up Approach with QuickTime*. Boston, MA: Wesley Addison Longman.

Angel, E. (2001b). *test second book by angel*. Boston, MA: Wesley Addison Longman.

Deussen, O., & Strothotte, T. (2000). Computer-generated pen-and-ink illustration of trees. *"Proceedings of" SIGGRAPH 2000*, (pp. 13–18).

Fisher, R., Perkins, S., Walker, A., & Wolfart, E. (1997). *Hypermedia Image Processing Reference*. New York, NY: John Wiley & Sons.

Gooch, B., & Gooch, A. (2001a). *Non-Photorealistic Rendering*. Natick, Massachusetts: A K Peters.

Gooch, B., & Gooch, A. (2001b). *Test second book by gooches*. Natick, Massachusetts: A K Peters.

Hertzmann, A., & Zorin, D. (2000). Illustrating smooth surfaces. *Proceedings of SIGGRAPH 2000*, *5*(17), 517–526.

Jain, A. K. (1989). *Fundamentals of Digital Image Processing*. Englewood Cliffs, New Jersey: Prentice-Hall.

Molina, S. T., & Borkovec, T. D. (1994). The Penn State worry questionnaire: Psychometric properties and associated characteristics. In G. C. L. Davey, & F. Tallis (Eds.), *Worrying: Perspectives on theory, assessment and treatment*, (pp. 265–283). New York: Wiley.

Noble, S. G. (2002). *Turning images into simple line-art*. Undergraduate thesis, Reed College.

Reed College (2007). Latex your document. `http://web.reed.edu/cis/help/LaTeX/index.html`

Russ, J. C. (1995). *The Image Processing Handbook, Second Edition*. Boca Raton, Florida: CRC Press.

Salisbury, M. P., Wong, M. T., Hughes, J. F., & Salesin, D. H. (1997). Orientable textures for image-based pen-and-ink illustration. *"Proceedings of" SIGGRAPH 97*, (pp. 401–406).

Savitch, W. (2001). *JAVA: An Introduction to Computer Science & Programming*. Upper Saddle River, New Jersey: Prentice Hall.

Wong, E. (1999). *Artistic Rendering of Portrait Photographs*. Master's thesis, Cornell University.